

NTS-926

Open File

Open File

UNITED STATES  
DEPARTMENT OF THE INTERIOR  
GEOLOGICAL SURVEY

Mail Stop 964, Federal Center, Box 25046  
Denver, Colorado 80225

Rock property analysis of core samples from the Calico Hills  
UE25a-3 borehole, Nevada Test Site, Nevada

by  
Lennart A. Anderson

Open-File Report 81-1337

1981

This report is preliminary and has not been reviewed for conformity with U.S. Geological Survey editorial standards. Any use of trade names is for descriptive purposes only and does not imply endorsement by the U.S.G.S.

Prepared by the U.S. Geological Survey  
for  
Nevada Operations Office  
U.S. Department of Energy  
(Memorandum of Understanding EW-78-A-0801543)

HYDROLOGY DOCUMENT NUMBER 70

## CONTENTS

	Page
Abstract-----	1
Introduction-----	1
Laboratory procedures for sample measurements-----	3
Laboratory results-----	10
Electrical measurements-----	10
Density measurements-----	18
Compressional sonic velocity-----	23
Magnetic properties-----	23
Summary-----	28
Selected reference-----	30

## ILLUSTRATIONS

	Page
Figure 1.--Map of the Nevada Test Site showing location of the Calico Hills UE25a-3 borehole-----	2
2.--Block diagram of instrumentation used for dc resistivity and induced polarization measurements-----	5
3.--Input and output signal waveforms at the current and potential electrodes of the sample holder used in the dc resistivity-induced polarization measurement-----	7
4.--Instruments and sample holder used for remanent magnetization measurements-----	9
5.--Resistivity values of natural-state and resaturated core samples plotted against depth of origin-----	13
6.--DC resistivity and induced polarization values plotted as a function of depth of origin-----	16
7.--Bulk density values for core samples plotted as a function of depth of origin-----	21
8.--Porosity and compressional sonic velocity values for borehole samples plotted as a function of depth of origin-----	24

ILLUSTRATIONS--Continued

	Page
Figure 9.--Remanent and induced magnetic intensities of borehole samples plotted with respect to depth of origin-----	27

TABLES

	Page
Table I.--Values of electrical resistivity and induced polarization for natural-state and saturated samples-----	11
II.--Values of natural bulk density (NBD), saturated bulk density (SBD), dry bulk density (DBD), grain density (GD), porosity, and compressional sonic velocity-----	19
III.--Values of remanent magnetic intensity ( $J_r$ ), magnetic susceptibility ( $K$ ), induced magnetization ( $J_i$ ), angle of remanent vector inclination ( $I_r$ ), and Koenigsberger ratio ( $Q$ )-----	25

ERRATA SHEET

Figure 2, page 5 - 0.2M KCL-silica gel should read: Gel made from fumed quartz and 0.2M KCL solution.

Rock property analysis of core samples from the Calico Hills

UE25a-3 borehole, Nevada Test Site, Nevada

by

Lennart A. Anderson

ABSTRACT

Core samples from the Calico Hills UE25a-3 borehole were measured for density, porosity, resistivity, induced polarization, compressional sonic velocity, and magnetic properties as part of the radioactive waste disposal site identification studies currently in progress at the Nevada Test Site. The samples were representative of three distinct subunits of argillite underlain by a marble section, all believed to be in the Mississippian part of the Eleana Formation. Because of a history of regional structural deformation, subsequent fracturing, and various degrees of fracture rehealing, the rock properties measured are highly variable within each principal rock section. Porosity changes affect virtually all rock properties measured except for magnetic intensity, and grain-density evidence shows that compositional differences are also a factor in producing the observed variability in rock properties. The induced polarization response is high in the argillite section owing to the concentration of pyrite, magnetite, and possible clay minerals within the fracture-filling material. The relatively high remanent and induced magnetization of the altered argillite subunit is a distinguishing feature of that section of argillite.

Introduction

Forty-nine core samples from the Calico Hills UE25a-3 borehole, located in the southwestern part of the Nevada Test Site (fig. 1), were obtained for measurement of selected rock properties as part of a large-scale site evaluation program intended to identify suitable underground repositories for radioactive

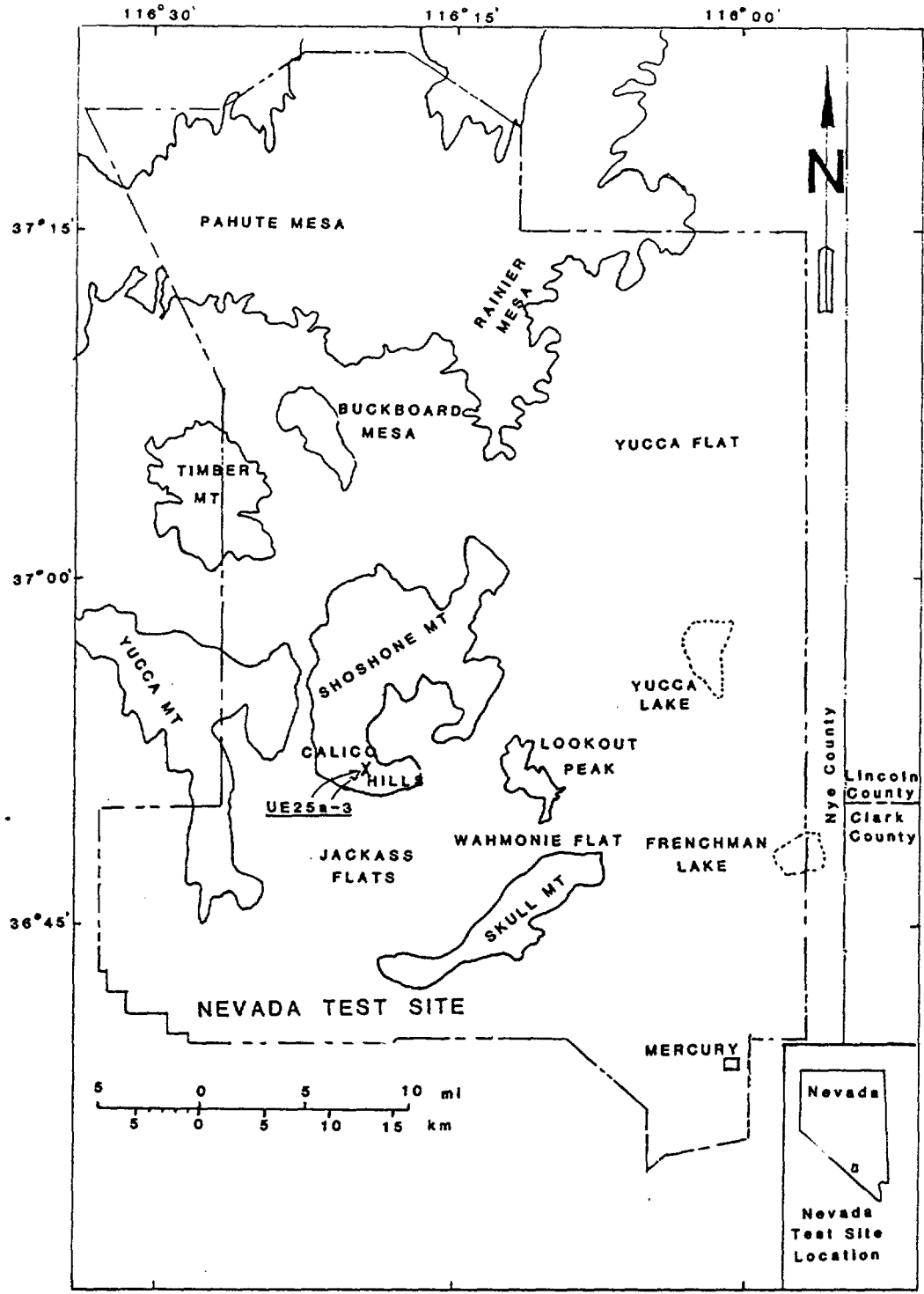


Figure 1. Map of the Nevada Test Site showing location of the Calico Hills UE25a-3 borehole.

waste products. The borehole was drilled to a depth of 771.2 m (2,530 ft), penetrating into unit J and possibly unit I of the Eleana Formation of Mississippian age (Maldonado and others, 1979). Unit J persists to the 720.6 m (2,364 ft) level and is primarily an argillite containing interbedded layers of quartzite, limestone, and siliceous sandstone. Below the 416.1 m (1,365 ft) depth the argillite has been thermally altered as the result of its proximity to an intrusive crystalline body believed to underlie the Calico Hills. That part of the section below the 720.6 m (2,364 ft) level, tentatively identified as unit I of the Eleana Formation, is marble crystallized from what was probably a dolomite by the intrusive body (Maldonado and others, 1979).

Upon extraction of core from the borehole, samples were selected so as to be representative of the significant lithologic variations observed within the major stratigraphic units. The cores were labeled for identification, wrapped in heavy aluminum foil, and coated with beeswax to preserve, as nearly as possible, the in situ conditions of the rock. Following delivery to the USGS Denver Laboratory facilities the samples were trimmed to uniform length and measured for electrical resistivity, induced polarization, porosity, bulk density, compressional seismic velocity, and remanent and induced magnetization. The results of the measurements are intended for use in the interpretation of inhole and surface geophysical surveys as well as to provide a means of rock property characterization not normally possible with conventional borehole techniques.

#### Laboratory procedures for sample measurements

The static water level in the borehole after completion of drilling was 639 m (2,096 ft), so it follows that a large portion of the core was taken from what may be the undersaturated zone. Because the degree of water saturation has a direct influence on such rock properties as resistivity and bulk density,

these properties were initially measured to determine their near in situ values. The samples, while still encased in beeswax, were cut to lengths of 6.35 cm (2.5 in) and unwrapped, cleansed superficially to remove the last vestiges of drilling mud, weighed, and then measured for electrical resistivity. Resistivity measurements were made at a frequency of 100 Hz using a four-terminal sample holder and a Hewlett-Packard digital LCR meter, model 4262A. The sample holder is simple in design: it consists of current and potential electrodes held apart from the core sample by a gel made from cab-o-sil silica and a 0.2 M solution of potassium chloride (figure 2). The gel as a conducting medium provides for an adequate current flow through the rock while contributing virtually nothing to the total resistance measured. The resistance (R) is read directly from the meter, and that value is multiplied by a geometric factor to obtain the resistivity ( $\rho$ ) of the sample such that  $\rho = AR/\ell$ . The geometric factor was determined from caliper measurements of diameter and length ( $\ell$ ) of the sample, from which the cross-sectional area (A) and volume were calculated. Volume was used in combination with sample weight to obtain what is herein referred to as natural bulk-density (NBD).

Following completion of the natural-state measurements, density and porosity values were determined using a method described by Johnson (1979). The samples were dried over a period of several days, weighed, and resaturated with tap water under a partial vacuum for a minimum time of 72 hours. The saturated samples were weighed in air and then weighed suspended in water. From these data, dry bulk density (DBD), saturated bulk density (SBD), grain density (GD), and fractional porosity ( $\phi$ ) were calculated as follows:

$$DBD = \frac{W_d}{V}, \quad (1)$$

where V is bulk rock volume obtained by a water displacement technique de-

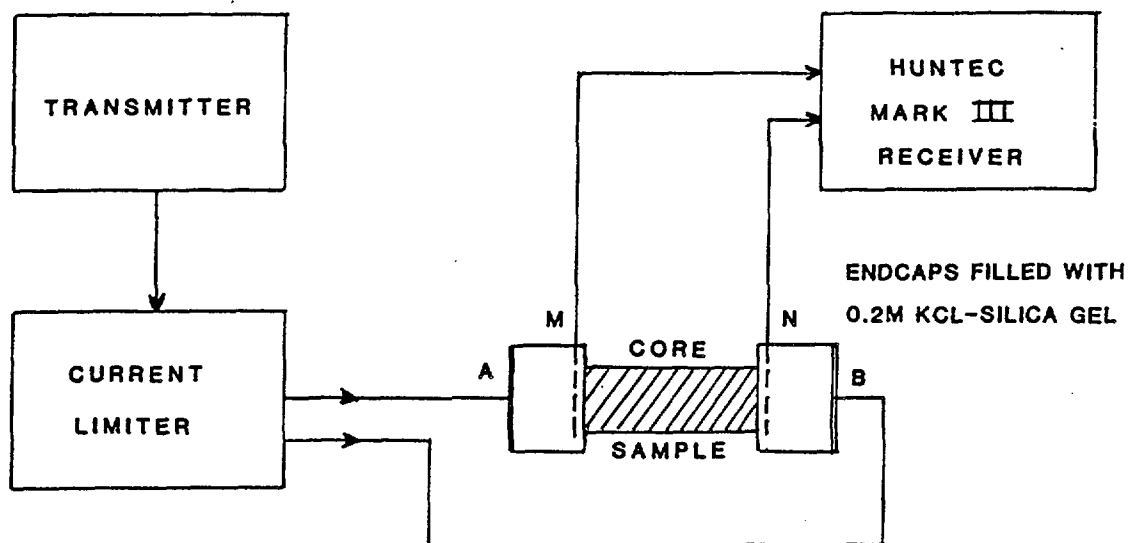


Figure 2. Block diagram of instrumentation used for dc resistivity and induced polarization measurements. A and B are the current electrodes, and M and N are the potential electrodes.

scribed by Chleborad and others (1975), and  $W_d$  is the dry weight of the sample;

$$SBD = \frac{W_s}{V}, \quad (2)$$

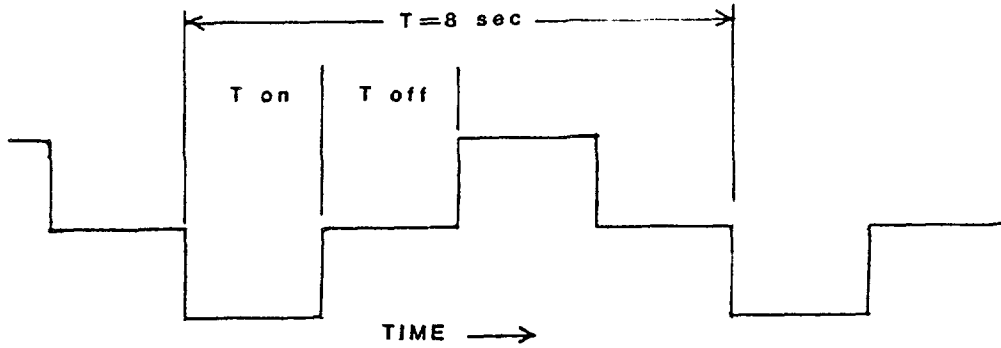
where  $W_s$  is the saturated weight of the sample;

$$\phi = \frac{W_s - W_d}{V}, \quad \text{and} \quad (3)$$

$$GD = \frac{Dd}{1 - \phi}. \quad (4)$$

While in the water-saturated state, the samples were remeasured for resistivity at 100 Hz as previously described. D.C. resistivity was also measured on resaturated samples in conjunction with induced polarization (I.P.), using the Huntec Mark III receiver and a custom-built transmitter (fig. 2). Current flow through the samples was controlled through a limiting device to avoid nonlinear effects in the I.P. response inherent in certain metallic and clay-bearing rocks. I.P. measurements were made in the time domain using the signal format shown in figure 3. During current flow the primary voltage across the potential electrodes is recorded together with the current for making resistivity determinations. Upon termination of current flow the transient decay voltage is integrated over the time interval  $T_p$  shown in figure 3 and normalized by the primary voltage such that induced polarization is read directly from the receiver as a dimensionless quantity, the ratio of the secondary to the primary voltage.

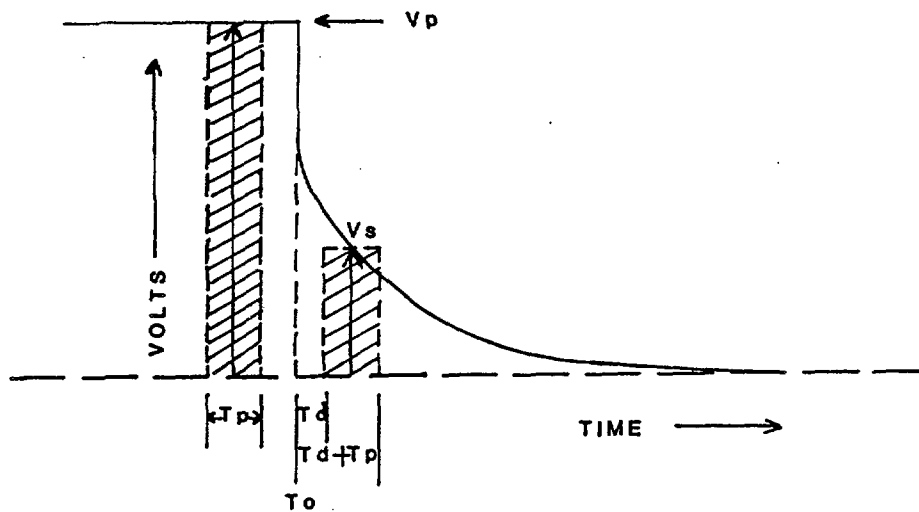
Compressional ultrasonic velocity measurements were made with a pulse technique as described by Obert and Duvall (1967). Prior to measurement the end surfaces of a core were lapped parallel to within 0.1 mm and the opposing faces coated with a thin layer of high-vacuum grease to assure good mechanical coupling between the sample and the bearing plates of the sample holder. The bearing plates contained piezoelectric transducers made of barium titanate



CURRENT WAVEFORM OUTPUT OF TRANSMITTER



SIGNAL WAVEFORM AT INPUT TO RECEIVER



EXPANDED VIEW OF RECEIVED SIGNAL SHOWING INTERVALS OF PRIMARY AND SECONDARY VOLTAGE MEASUREMENT

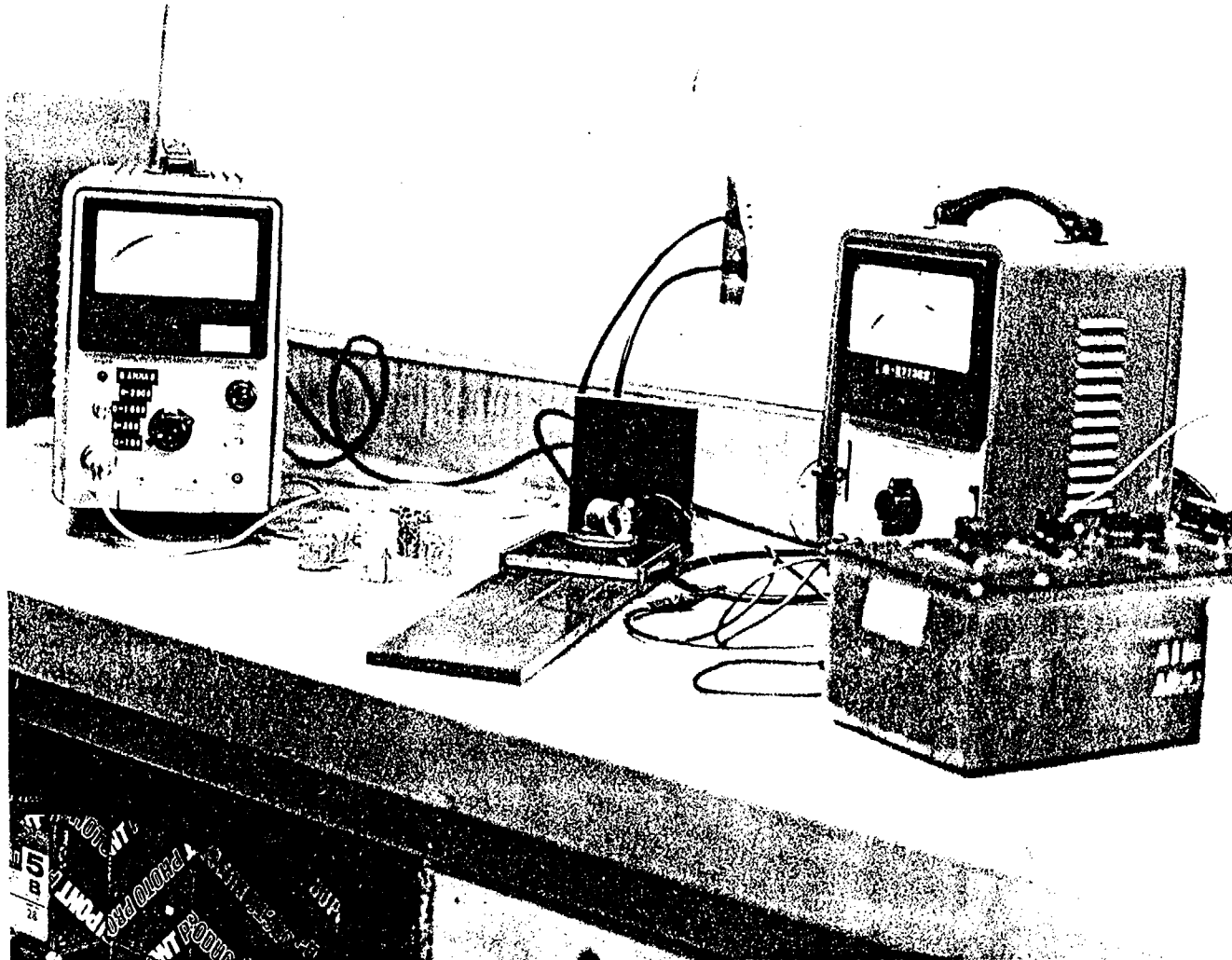
Figure 3. Input and output signal waveforms at the current and potential electrodes of the sample holder used in the dc resistivity-induced polarization measurement. The lowermost waveform indicates the signal sampling intervals for the primary voltage ( $V_p$ ) and the transient voltage ( $V_s$ ).  $T_p$  is the integrating time for both  $V_p$  and  $V_s$ , which in this instance was 30 milliseconds. The time delay ( $T_d$ ) following termination of current flow and transient voltage measurement was 15 milliseconds.

crystals held in mechanical contact with the sample for energy transmission and detection. The transmission crystal converts a high-voltage pulse of less than 10  $\mu$ s duration to a compressional wave which is propagated through the sample, detected, and reconverted to a voltage pulse at the receiver crystal. Both transmitted and received pulses are displayed on an oscilloscope, and, by means of a calibrated time delay circuit, the time difference between pulses is readily resolved.

Traveltime measurements were also made using 40-mm-diameter aluminum rods, 50 to 90 mm in length, to determine system delay time. The plot of traveltime vs. rod length was extended to the zero line intercept to derive the value used as a correction factor in the final calculation of sample acoustic velocity.

Precise measurements of remanent magnetization and magnetic susceptibility are normally made with sophisticated instruments designed to accept a sample cut to a specific size. Because of the fragile nature of the Eleana Formation samples, however, it was considered prudent to measure these magnetic properties by using simpler types of instruments which obviate the need for sample reshaping, but, in so doing, some sensitivity and subsequent resolution in individual measurements was sacrificed.

The method used for remanent magnetization is described in Jahren and Bath (1967); it has the capability of determining magnetic directions within 10 degrees and intensities within 6 percent as compared with standard laboratory techniques. Figure 4 is a photograph of an equivalent setup. A calibration constant is used in conjunction with static measurements of sample magnetization in the x, y, and z directions to compile a magnetic vector, assuming that the in situ orientation of the sample is known. In the case of the Calico Hills core only the vertical attitude is known, and therefore the parameter determinations were limited to remanent magnetic intensity and inclination.



6

Figure 4. Instruments and sample holder used for remanent magnetization measurements. The Hewlett-Packard milliammeter Model 628A on the left is fitted with a fluxgate probe leading to the custom-built sample holder in the center of the photo. The white dot on the back panel of the sample holder is the detector end of the sensor shown in relation to the rotating platform on which a calibration coil is resting. The coil is energized with a dc current controlled by the resistance box on the right and indicated on the dc milliammeter adjacent to the resistance box.

Magnetic susceptibility measurements were made with an alternating current mutual inductance bridge (Bruel and Kjaer, Deviation Test Bridge, Type 1502), and two air-core coils of the helmholtz type. One coil is used to obtain an approximate balance on the galvanometer by varying the distance between the windings on the coil. A sample is introduced into the second coil, and the resulting imbalance is read directly from the galvanometer and converted to magnetic susceptibility by means of a calibration factor established through the use of known susceptibility standards.

#### Laboratory results

According to Maldonado and others (1979), because of faulting, jointing, brittleness, and intensity of alteration and brecciation, 67 percent of the rock intersected in the drill hole is considered to be incompetent. A fragile character is implied for the entire cored section, necessitating careful handling of those core sections selected for laboratory study. The process of wrapping and encasing the sample in a thick covering of beeswax upon removal from the borehole served to keep the sample in one piece, and, equally important, the beeswax coating assured that the waters within the pore spaces of the rock were contained, allowing resistivity and bulk density measurements to be made so as to obtain values most representative of natural state conditions.

Electrical Measurements: The result of the total number of resistivity and induced polarization measurements made are listed in Table 1. Resistivities measured at 100 Hz for natural-state and resaturated samples are plotted in figure 5 with respect to their depth of origin. The number of data points was greatest for the natural-state sample suite and therefore these points are shown connected by a broken line intended to serve as a visual aid in describing resistivity variation with depth rather than to imply a uniform resistivity interval between data points. Corresponding data for resaturated samples are

TABLE I

Values of electrical resistivity and induced polarization for natural state and saturated samples.  
[Leader (-) indicates no measurement possible]

Sample depth in feet (meters)	100-Hz resistivity in ohm-m		dc resistivity in ohm-m (saturated)	Induced polarization in percent
	Natural state	Saturated		
128 (39)	32	-	-	-
216 (65.9)	3970	863	1035	52
282 (86)	228	-	-	-
285 (86.9)	-	-	-	-
295 (89.9)	-	-	-	-
302 (92.1)	129	-	-	-
332 (101.2)	55	-	-	-
354 (107.9)	106	67	59	2
420 (128.1)	30	-	-	-
550 (167.7)	86	-	-	-
586 (178.7)	120	-	-	-
643 (196)	-	-	-	-
666 (203)	158	130	142	17
676 (206.1)	104	-	-	-
713 (217.4)	359	206	213	2
753 (229.6)	84	79	105	78
866 (264)	277	-	-	-
932 (284.2)	87	80	85	7
994 (303.1)	86	-	-	-
1041 (317.4)	359	-	-	-
1229 (374.7)	243	-	-	-
1282 (390.9)	312	-	-	-
1317 (401.5)	183	-	-	-
1393 (424.7)	1052	968	1067	10
1427 (435.1)	166	141	151	10
1448 (441.5)	819	640	755	19
1518 (462.8)	235	231	233	3
1553 (473.5)	3875	1276	1410	22
1598 (487.2)	229	214	227	27

TABLE I - continued

Sample depth feet (meters)	100-Hz resistivity in ohm-m		dc resistivity in ohm-m (saturated)	Induced polarization in percent
	Natural state	Saturated		
1649 (502.7)	8680	11704	226	3
1675 (510.7)	376	262	331	15
1721 (524.7)	1064	1100	1240	12
1736 (529.3)	118	120	135	10
1820 (554.9)	153	158	166	5
1961 (599.7)	347	390	444	14
2009 (612.5)	513	431	523	6
2076 (632.9)	394	383	498	14
2125 (647.9)	806	-	-	-
2150 (655.5)	555	515	539	12
2241 (683.2)	199	190	195	7
2300 (701.2)	-	-	-	-
2342 (714)	dry	580	811	37
2371 (722.9)	574000	14970	14700	7
2380 (725.6)	385	460	454	8
2406 (733.5)	4665	3290	6615	1
2465 (751.5)	8685	6750	3920	2
2523 (769.2)	9531	1980	2190	1

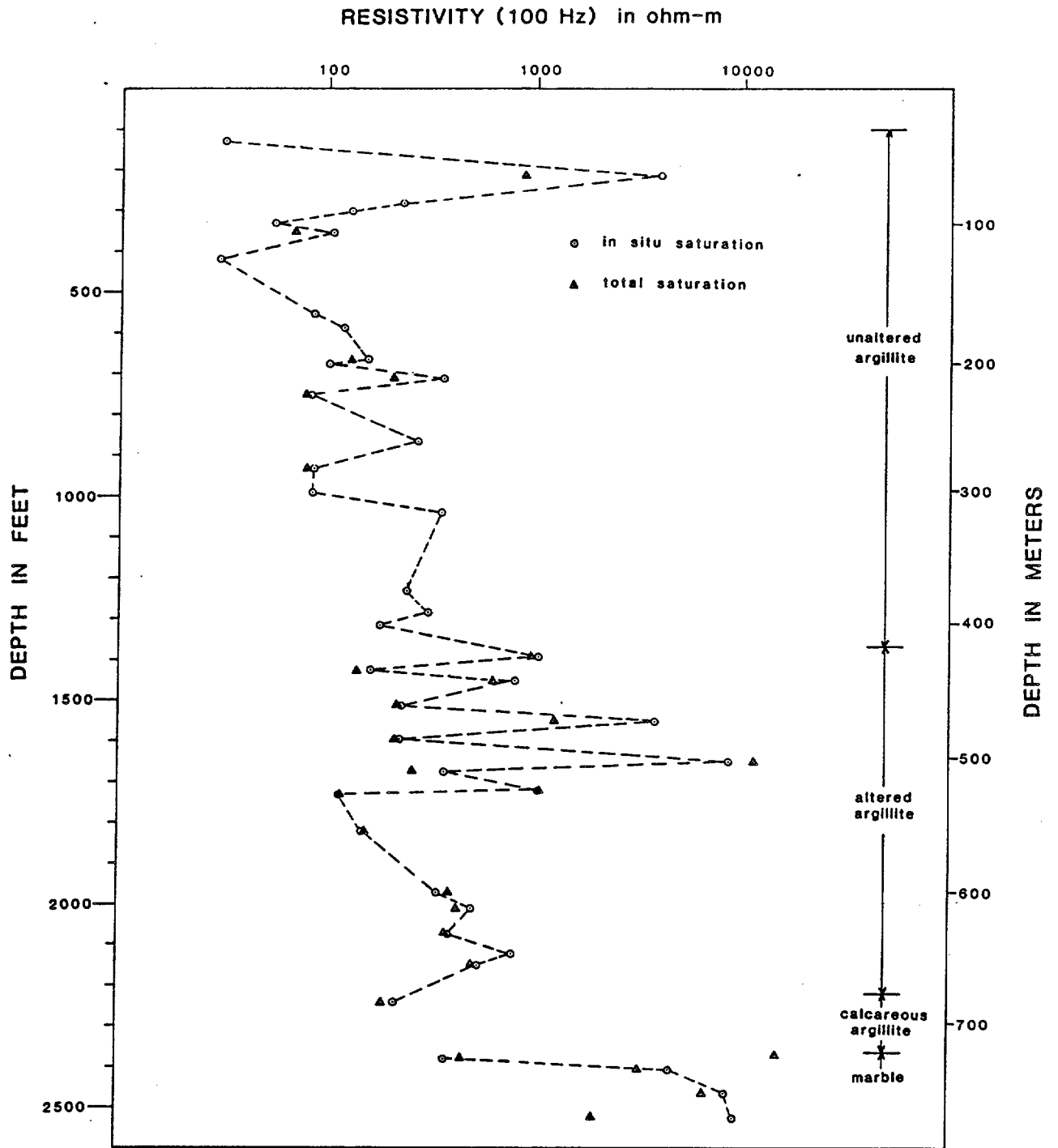


Figure 5- Resistivity values of natural-state and resaturated core samples plotted against depth of origin. Dashed line connects the natural state data points to demonstrate resistivity variations with depth.

fewer because of the losses resulting from the resaturation process primarily affected those samples from the most heavily fractured and least competent sections encountered in the borehole.

In virtually every instance where values can be compared, the natural-state sample resistivities are higher than those of the resaturated samples. This result is not totally unexpected because, above some critical level of water content, the bulk resistivity of rock is known to vary inversely with the fraction of total pore volume filled with water. There is no pattern to differences in resistivity within any particular interval where dual measurements exist. Many natural-state and fully saturated resistivity values are very nearly the same, indicating that the larger resistivity differences are possibly caused by pore-water evaporation occurring between the time of core removal from the borehole and the time at which the sample was sealed. A clue to the degree of water loss should normally be provided from observations on resistivity differences noted on those samples taken from below the standing water level. However, these samples had been used for other purposes which necessitated the breaking of the beeswax coating and, as a result, were probably somewhat dehydrated and therefore not truly representative of in situ saturation levels.

The resistivity values for lithologic components of the Eleana Formation range from tens of ohm-meters for argillaceous argillite to thousands of ohm-meters for limestone sections, and values for quartzite fall between the two extremes (Anderson and others, 1980). Based on this correlation the resistivity plot in figure 5 can be used to formulate some notion as to the rock type encountered within the borehole, although it is recognized that textural variations and the degree of fracturing can modify resistivities to the extent that the inferred relationship may be somewhat obscured.

The rapid changes in resistivity within the borehole attest to the high

degree of stratification of the rock column. This effect is particularly evident in the upper part of the altered argillite subunit in the 414.6-530.5 m (1360-1740 ft) interval, where intercalated limestones, quartzites, and thermally altered argillites produce a highly irregular resistivity pattern within a relatively short interval. The background resistivity level of the altered argillite is perceptibly higher than that of the unaltered section, possibly a result of the greater quartz content in the altered argillites (Maldonado and others, 1979). The resistivities of the two samples representing the calcareous altered argillite are very similar to those of the overlying altered argillite, making it difficult to distinguish between the subunits on the basis of their resistivity. The quartz content of the calcareous section reportedly varies from 10 to 60 percent, and therefore the resistivities may be expected to vary to a greater extent than otherwise indicated by the sample measurements.

With one exception the marbles of the lowermost unit have very high resistivities. The sample taken from the 725.6 m (2380 ft) depth level has an appreciably higher porosity than that of the other marbles and consequently, has a higher water content resulting in a proportionately lower resistivity.

Resistivities and induced polarization data obtained on saturated samples with the Huntect receiver at a very low frequency are listed in Table 1 and are shown plotted against depth on figure 6. For the most part the near d.c. resistivities are slightly higher than those measured at 100 Hz because of the frequency-dependent dielectric constant of the rock, but, where significant resistivity differences occur, electrochemical polarization is the primary cause. At the current density levels used in generating an I.P. response, the principal phenomenon involved is that of concentration overvoltage--the double-layer effect

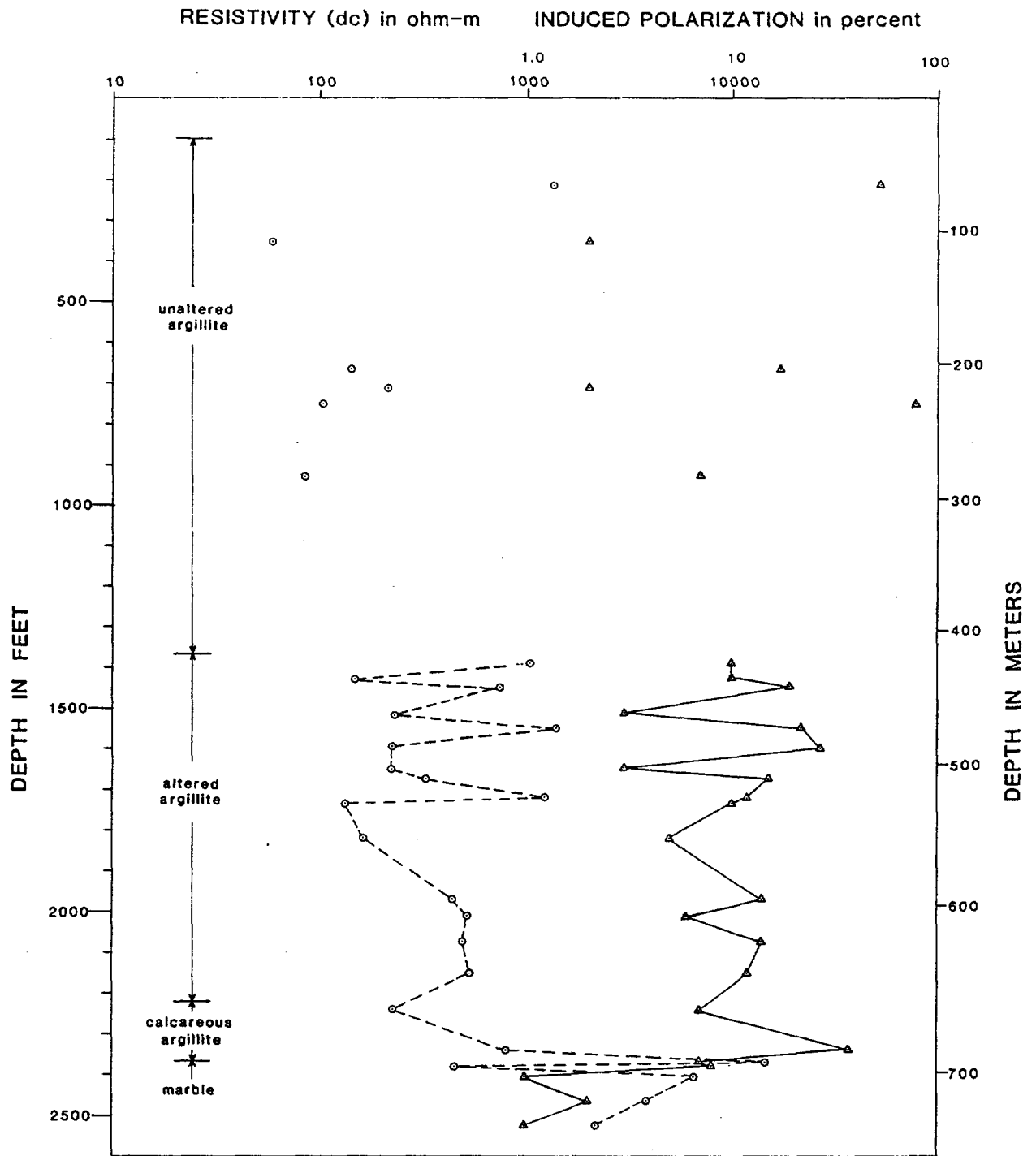


Figure 6. DC resistivity and induced polarization values plotted as a function of depth of origin. Resistivity values, shown as circles, and induced polarization values, shown as triangles, are connected by dashed and solid lines, respectively, where the data are closely spaced to show variations with depth. The solid line is not intended to imply continuity between data points.

mentioned in Sumner (1976). This type of polarization is brought about by the accumulation of ions in the pore waters near the surfaces of metallic mineral grains contained within the rock. Ion accumulation occurs during the time of current flow, and, upon termination of the energizing current, the unbound ions of like charge diffuse from the zones of concentration, giving rise to a transient voltage from which the I.P. response of the rock is calculated.

In the unaltered argillite those samples having polarization values in excess of 10 percent show clear evidence of pyrite within the fractures of the rock. Pyrite, an excellent polarizer, occurs either singly or interlaced with other fracture-filling materials. Magnetite, a comparatively poor polarizer, exists in sufficient quantities within the altered argillite to produce a high background level of polarization. In those samples having low I.P. values, magnetite is found only within the fractures of the rock; but in those samples that have higher polarization values, magnetite can also be found disseminated throughout the rock in the form of poorly concentrated blebs or bands.

Although there are only two samples representing the relatively thin calcareous argillite section underlying the altered argillite, the I.P. response is on the order of that measured for altered argillite. Magnetic property determinations support the observation that there is no magnetite in the calcareous section, nor is there any evidence of the existence of other metallic minerals within the rock. According to Maldonado and others (1979), there is very little difference in the rock mineralogy between the three subunits of argillite except that the predominant clay in the calcareous argillite is corrensite, whereas illite is predominant in the unaltered and altered argillite, though it is mixed with lesser quantities of montmorillonite in the latter. Clay minerals can produce a polarization response through a mechanism called membrane polarization, which is similar to electrode polarization except that ion accumulation occurs

within the electrolyte in the vicinity of a charged clay particle during current flow (Sumner, 1976). The diffusion process is much the same as in electrode polarization except that the transient voltage produced by membrane polarization is usually much smaller. However, depending upon rock texture and upon the volume fraction, distribution, and type of clay contained within the rock, appreciable polarization values can be realized. It is not certain that corrensite in a calcareous argillite can produce I.P. values of the amplitude measured on samples from that section, but there is no other apparent explanation.

The I.P. of the lowermost marble subunit varies from above normal background level to the upper zone to a very low I.P. response in the most competent lower zone. Maldonado and others (1979) report the existence of magnetite within the fractures of the marbles of the upper zone, but magnetic evidence shows that the magnetite must be sparse. Possibly clay minerals contribute to the total I.P. amplitude of samples having high polarization values in the marble section.

Density measurements: Samples were measured for natural bulk density (NBD), saturated bulk density (SBD), dry bulk density (DBD), grain density (GD), and porosity ( $\phi$ ), the latter calculated from density and volume determinations. These data are listed in Table II, which also includes the measured values of compressional sonic velocity. The NBD, DBD, and SBD data are plotted against depth of sample origin in figure 7 to illustrate variations in density as a function of water content. For those samples allowing comparisons, there are obvious differences between the sets of density determinations that are most pronounced in those samples having the higher porosities. The density variations indicated by the connecting line drawn through the NBD data points are maintained for each density data set. Therefore the NBD graph can probably be taken as a definitive plot of the manner with which textural changes occur within the penetrated rock section.

TABLE II

Values of natural bulk density (NBD), saturated bulk density (SBD), dry bulk density (DBD), grain density (GD), porosity, and compressional sonic velocity. [Leader (-) indicates no measurement possible]

Sample depth in feet (meters)	NBD <sub>3</sub> Mg/m <sup>3</sup>	SBD <sub>3</sub> Mg/m <sup>3</sup>	DBD <sub>3</sub> Mg/m <sup>3</sup>	GD <sub>3</sub> Mg/m <sup>3</sup>	Porosity in percent	Compressional sonic velocity km/sec
128 (39)	2.43	-	-	-	-	-
216 (65.9)	2.61	2.66	2.61	2.73	4.4	4.87
282 (86)	2.58	-	-	-	-	-
285 (86.9)	-	-	-	-	-	-
295 (89.9)	2.5	-	-	-	-	-
302 (92.1)	2.55	-	-	-	-	-
332 (101.2)	2.56	-	-	-	-	-
354 (107.9)	2.56	2.58	2.50	2.72	8.2	-
420 (128.1)	2.63	-	-	-	-	-
550 (167.7)	2.55	-	-	-	-	-
586 (178.7)	2.57	-	-	-	-	-
643 (196)	-	2.58	2.48	2.75	9.8	-
666 (203)	2.57	2.62	2.55	2.75	7.3	-
676 (206.1)	2.58	2.55	2.43	2.76	11.8	-
713 (217.4)	2.62	2.65	2.57	2.78	7.5	2.81
753 (229.6)	2.59	2.61	2.52	2.77	9.0	2.71
866 (264)	2.63	2.64	2.58	2.74	6.2	-
932 (284.2)	2.50	2.57	2.45	2.77	11.3	2.3
994 (303.1)	2.57	-	-	-	-	-
1041 (317.4)	2.60	-	-	-	-	-
1229 (374.7)	2.63	-	-	-	-	-
1282 (390.9)	2.65	2.61	2.52	2.77	9.1	-
1317 (401.5)	2.59	2.60	2.49	2.81	11.5	-
1393 (424.7)	2.59	2.61	2.56	2.69	5.0	4.77
1427 (435.1)	2.50	2.54	2.42	2.74	11.7	3.61
1448 (441.5)	2.40	2.47	2.35	2.66	11.5	4.92
1518 (462.8)	2.53	2.56	2.46	2.72	9.8	4.17
1553 (473.5)	2.58	2.61	2.55	2.71	5.8	3.14
1598 (487.2)	2.49	2.54	2.43	2.74	11.4	4.47
1649 (502.7)	2.60	2.62	2.60	2.66	2.3	5.23

TABLE II - continued

Sample depth in feet (meters)	NBD <sub>3</sub> Mg/m <sup>3</sup>	SBD <sub>3</sub> Mg/m <sup>3</sup>	DBD <sub>3</sub> Mg/m <sup>3</sup>	GD <sub>3</sub> Mg/m <sup>3</sup>	Porosity in percent	Compressional sonic velocity km/sec
1675 (510.7)	2.46	2.48	2.34	2.72	13.9	2.20
1721 (524.7)	2.61	2.63	2.58	2.72	4.9	4.50
1736 (529.3)	2.40	2.42	2.25	2.72	17.2	3.23
1820 (554.9)	2.51	2.54	2.43	2.72	10.8	4.18
1969 (599.7)	2.56	2.63	2.56	2.74	6.6	4.8
2009 (612.5)	2.52	2.57	2.52	2.64	4.4	4.5
2076 (632.9)	2.47	2.50	2.39	2.68	10.9	4.37
2125 (647.9)	2.13	2.35	2.12	2.74	22.6	-
2150 (655.5)	2.53	2.56	2.49	2.69	7.5	5.97
2241 (683.2)	2.53	2.55	2.44	2.72	10.1	4.55
2300 (701.2)	-	-	-	-	-	-
2342 (714)	dry	2.55	2.49	2.64	5.8	4.91
2371 (722.9)	2.69	2.72	2.71	2.75	1.3	6.50
2380 (725.6)	2.38	2.50	2.34	2.79	16.2	4.21
2406 (733.5)	2.49	2.58	2.56	2.63	2.6	5.83
2465 (751.5)	2.59	2.61	2.57	2.64	2.6	6.08
2523 (769.2)	2.45	2.52	2.45	2.65	7.6	5.26

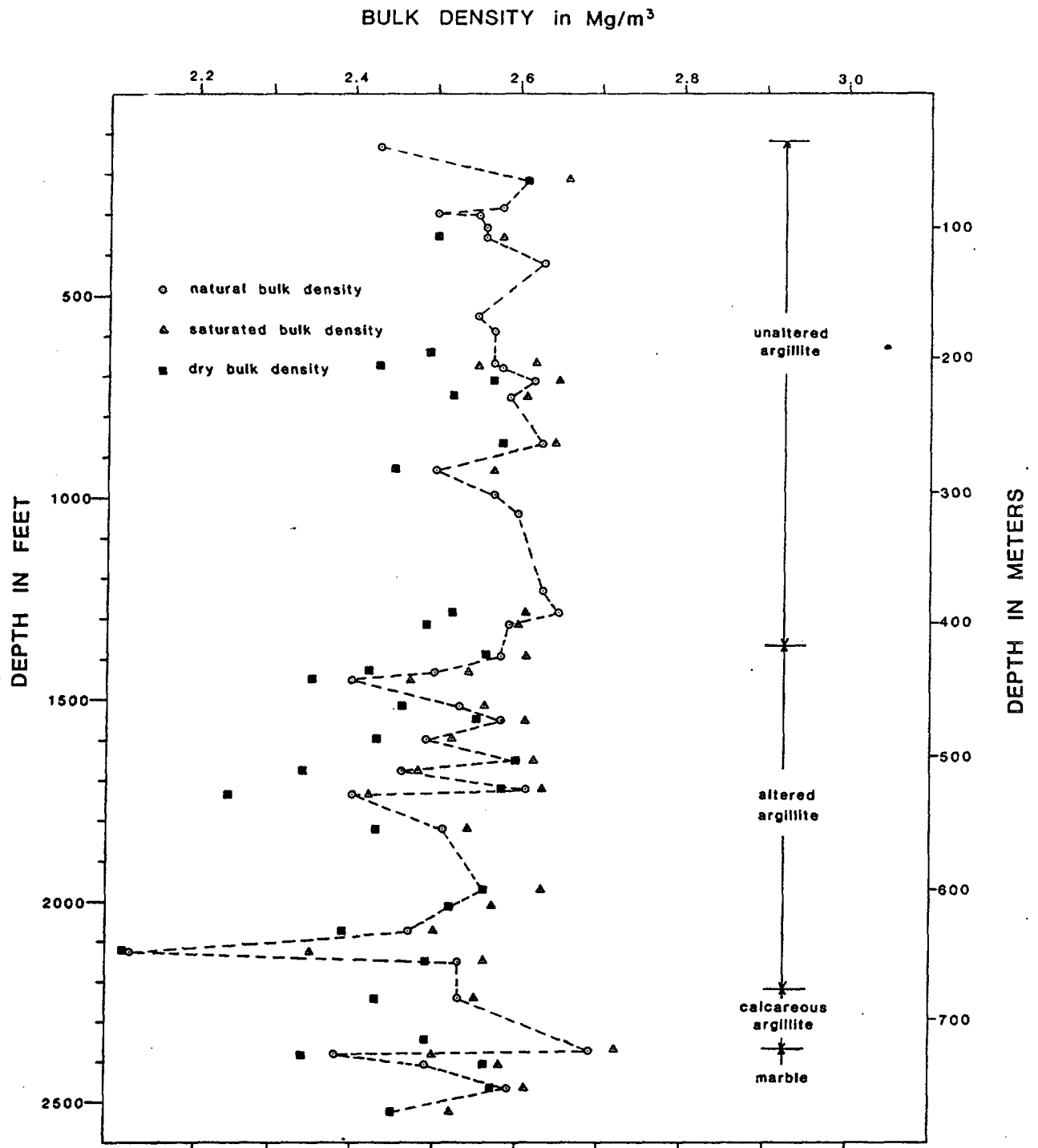


Figure 7. Bulk density values for core samples plotted as a function of depth of origin. The dashed line connects natural bulk density values to aid in demonstrating variations with depth.

Typically, the NBD values fall somewhere between the DBD and SBD values. As noted in the resistivity section, those samples taken from below the water table and thus expected to be totally saturated indicate partial saturation. Therefore it is apparent that the samples have been dehydrated to some extent after the core was extracted from the borehole, possibly during the time of thermal conductivity measurements made earlier in Menlo Park, Calif. As a consequence, there is no precise measurement of NBD on samples containing in situ levels of water saturation. Except for the uppermost part of the section, where transpiration and seasonal fluctuations in rainfall cause periodic variations in the pore water content of the rock, it is assumed that the SBD values most nearly approximate those of the in-place rocks.

Grain densities of the three argillite subunits are reasonably uniform, indicating only subtle differences in the composition of the argillite. Based on published density ranges for common rock types (Johnson and Olhoeft, 1981), the lowest grain densities can be correlated with calcareous argillite and the highest with quartzitic argillite. However, the effect of compositional variations on the bulk density of the argillites is negligible compared to that of porosity. As an example, the grain density of the core taken from 648 m (2125 ft) is  $2.74 \text{ Mg/m}^3$  which is  $0.02 \text{ Mg/m}^3$  greater than the mean value determined for the argillite sections, but the saturated bulk density is  $2.35 \text{ Mg/m}^3$ , the lowest for all samples measured. The porosity of that sample, which includes both fracture and intergranular porosity, is accordingly 22.6 percent, the highest determined for all samples. Similar examples of the effect of porosity on bulk density are apparent from comparative values listed in Table II.

On an average, the marble samples have grain densities significantly lower than those of the argillites. Nevertheless, the bulk densities are similar to those of the argillites, which is a reflection of low porosity of the marble.

### Compressional sonic velocity

Compressional sonic velocities measured on water-saturated samples are shown plotted along with porosity as a function of depth of origin in figure 8. Very few measurements were possible on the unaltered argillite samples because of the fragile nature of the rock. Below the 427 m (1400 ft) level the variability in both porosity and compressional velocity attests to the changing character of the rock, particularly within the altered argillite section. The velocity shows an inverse dependence upon porosity, but the relationship is not well defined. Other properties of the rock, such as its grain size, lithification, and chemical composition, also have some influence on the seismic velocity. Average velocities increase with depth of burial, possibly reflecting a higher degree of lithification and a difference in the chemical composition of the rock.

### Magnetic properties

Magnetic susceptibility and remanent magnetization measurements were made on as many samples as possible following their removal from their protective coating. The plotted and tabulated results (figure 9 and Table III) include the calculated values of the induced magnetization and Koenigsberger's ratio in SI units. The results include a reasonably representative number of data points and serve to illustrate differences in the magnetic character of the three argillite units and the marble section. On figure 9, major gaps in the data plot represent sections of core that were particularly fragile and easily disintegrated in the course of handling.

A comprehensive study of the magnetic properties of samples from the Calico Hills UE25a-3 borehole has been made by M. J. Baldwin and C. E. Jahren (written commun., 1981). Their work involved a greater number of samples and was somewhat directed towards resolving the problem of the near-vertical inclinations of the remanent magnetization, which applies particularly to samples from the altered argillite section. By degaussing these samples in fields of 200 Oe or less,

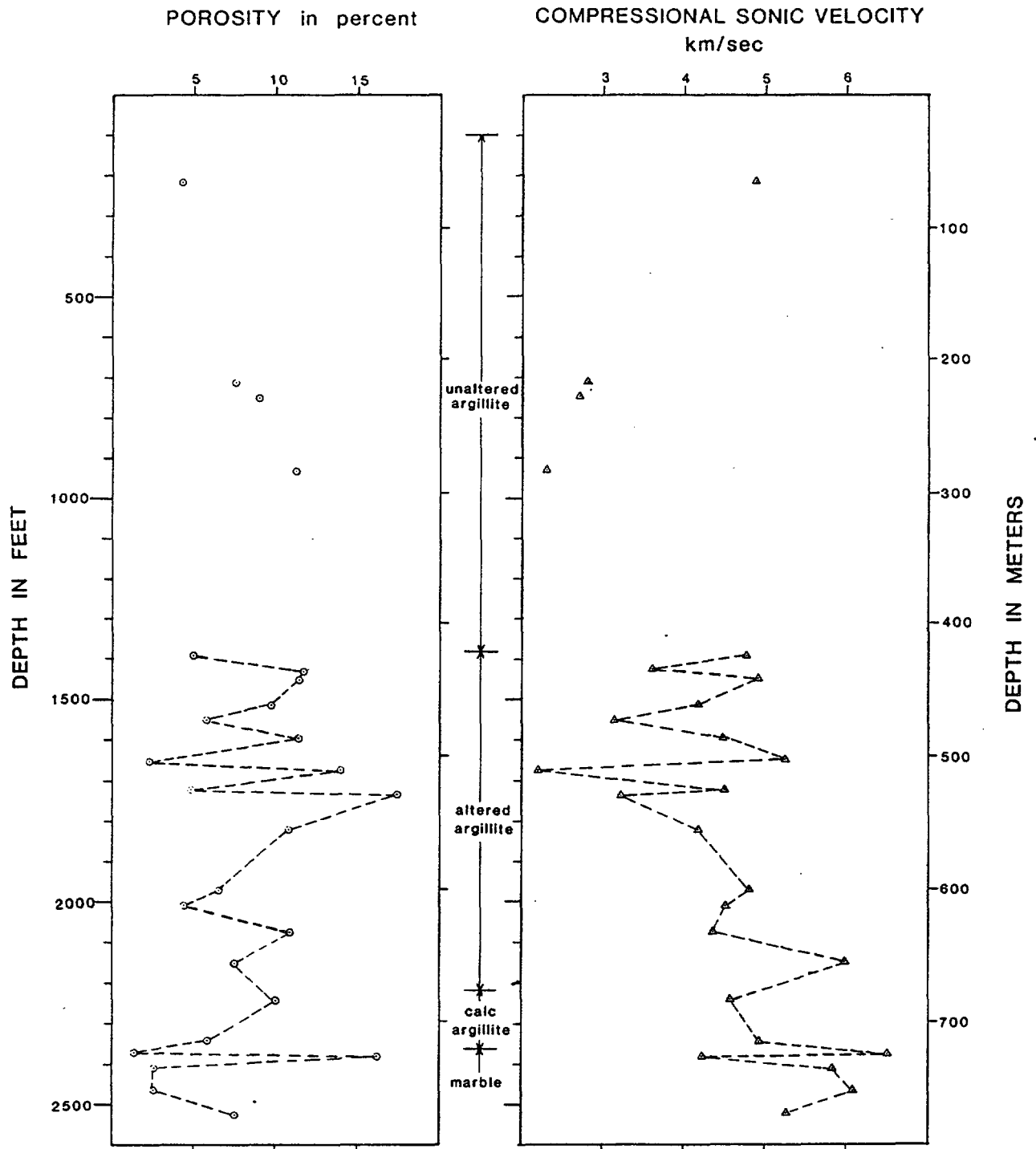


Figure 8. Porosity and compressional sonic velocity values for borehole samples plotted as a function of depth of origin. Data points are connected by dashed lines where closely spaced to show variation with depth.

TABLE III

Values of remanent magnetic intensity (Jr), magnetic susceptibility (K), induced magnetization (Ji), angle of remanent vector inclination (Ir), and Koenigsberger ratio (Q)  
 [Leader (-) indicates no measurement possible]

Sample depth in feet (meters)	Jr amp/m	Kx10 <sup>3</sup> in MKS units	Ji amp/m	Ir Degrees	(Q)
128 (39)	0.029	0.50	0.021	40	1.4
216 (65.9)	0.034	0.137	0.0057	47	6.1
282 (86)	-	-	-	-	-
285 (86.9)	-	-	-	-	-
295 (89.9)	-	-	-	-	-
302 (92.1)	0.023	0.308	0.013	50	1.8
332 (101.2)	-	-	-	-	-
354 (107.9)	0.024	0.44	0.018	20	1.3
420 (128.1)	-	-	-	-	-
550 (167.7)	-	-	-	-	-
576 (178.7)	-	-	-	-	-
643 (196)	-	-	-	-	-
666 (203)	0.023	0.779	0.032	21	0.7
676 (206.1)	0.025	0.156	0.0065	10	3.9
713 (217.4)	0.015	0.565	0.023	22	0.6
753 (229.6)	0.028	0.302	0.012	30	2.2
866 (264)	0.033	0.402	0.017	41	2.0
932 (284.2)	0.044	0.59	0.024	63	1.8
994 (303.1)	0.150	1.24	0.051	76	2.9
1041 (317.4)	0.024	0.565	0.023	16	1.0
1229 (374.7)	-	-	-	-	-
1282 (390.9)	1.24	0.167	0.0069	51	179.4
1317 (401.5)	1.12	14.2	0.59	78	1.9
1393 (424.7)	0.080	0.358	0.015	58	5.4
1427 (435.1)	0.155	2.48	0.10	73	1.5
1448 (441.5)	0.797	10.3	0.43	75	1.9
1518 (462.8)	1.43	17.1	0.71	66	2.0
1553 (473.5)	6.1	22.6	0.94	63	6.5
1598 (487.2)	-	-	-	-	-

TABLE III - continued

Sample depth in feet (meters)	Jr amp/m	$K \times 10^3$ in MKS units	Ji amp/m	Ir Degrees	(Q)
1649 (502.7)	1.08	3.27	0.14	75	8.0
1675 (510.7)	3.0	8.73	0.36	84	8.3
1721 (524.7)	8.15	15.8	0.65	66	12.4
1736 (529.3)	1.49	3.77	0.16	75	9.6
1820 (544.9)	0.871	3.52	0.15	79	6.0
1967 (599.7)	-	-	-	-	-
2009 (612.5)	3.35	7.29	0.30	84	11.1
2076 (632.9)	1.98	2.69	0.11	88	17.8
2125 (647.9)	4.31	7.69	0.32	88	13.5
2150 (655.5)	3.84	7.29	0.30	80	12.7
2241 (683.2)	0.443	0.904	0.037	88	11.8
2300 (701.2)	-	-	-	-	-
2342 (714)	0.039	1.03	0.043	71	0.9
2371 (722.9)	-	-	-	-	-
2380 (725.6)	0.020	0.231	0.0096	73	2.1
2406 (733.5)	0.016	0.981	0.041	42	0.4
2465 (751.5)	-	0.231	0.0096	-	-
2523 (769.2)	-	0.231	0.0096	-	-

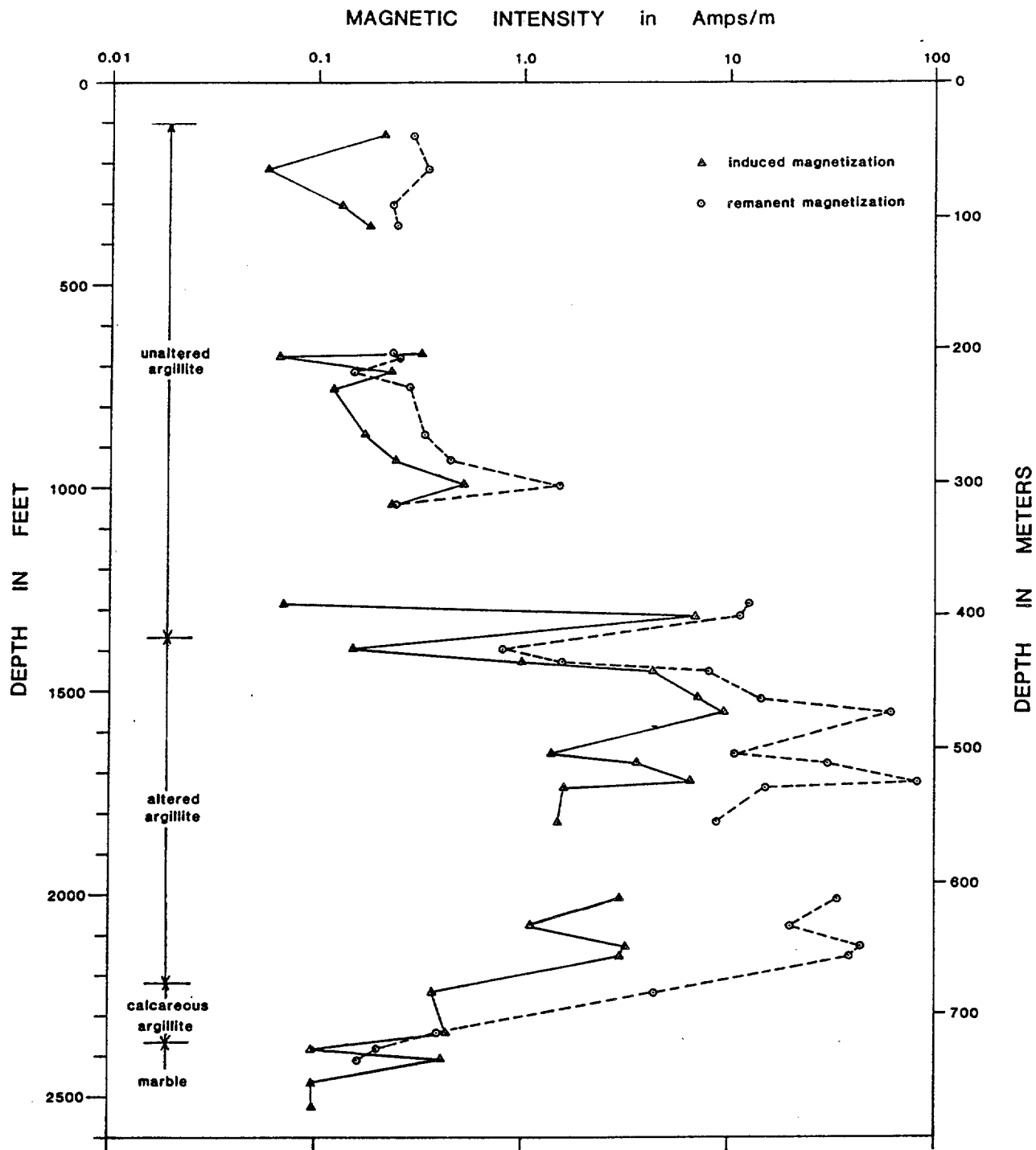


Figure 9. Remanent and induced magnetic intensities of borehole samples plotted with respect to depth of origin. Lines drawn between data points show variations in magnetic values with depth. In those sections where the lines have been discontinued the core samples were found to be particularly fragile.

a "soft" component of remanence was removed and an inclination more in line with the present day Earth's magnetic field inclination of  $62^{\circ}$  was finally realized. Baldwin and Jahren speculate on the probability that the "soft" component of remanent magnetization has been emplaced within the sample as a result of remagnetization that occurred during the drilling operation. Based on their findings, it is apparent that the inclinations of the remanent vectors ( $I_r$ ) listed in Table III are not valid for the altered sections and perhaps not for the calcareous argillite sections either.

The data plot on figure 9 shows the intensities of the remanent and induced components of magnetization of the altered argillite to be substantially higher than those of the adjoining rock section. As indicated in the discussion on induced polarization, magnetite as fracture-filling material and as inclusions in the groundmass of the rock is the cause of the increased magnetization.

Table III also lists values for the Koenigsberger ratio,  $Q$ , which is the remanent magnetic intensity divided by the product of magnetic susceptibility and the inducing field. At NTS, the inducing field has an intensity of 41.38 amp/m. The Koenigsberger ratio is significant because it can be used to obtain an estimate of the relative importance of remanent and induced magnetization as contributing elements in the generation of magnetic anomalies. In those rocks measured the remanent component generally predominates, but their orientation is invariably aligned with the present day Earth's field. Therefore the remanent and induced components are additive and should produce no complex magnetic patterns as viewed from the surface.

#### Summary

The most complete data sets obtainable were those of bulk density and resistivity acquired during the first round of measurements on the freshly unwrapped samples, which contained amounts of water nearly equal to the in-place

pore waters. Although it is evident that the cores as received were not totally water saturated, where multiple measurements of the same type on a single sample were possible, the similar pattern of variation noted in both resistivity and density values suggests that the character of the textural and compositional changes within the penetrated section is preserved in the plots of the original data sets.

The bulk densities of the unaltered argillite samples are reasonably uniform, indicating minimal compositional differences within this subunit. Variations in both resistivity and density are believed to be caused by porosity changes, which are related to fracture density and the extent to which the fractures have been sealed by mineral precipitates. The altered argillite, structurally more competent than the unaltered argillite, varies appreciably in texture and composition, particularly in the upper half of the section, where the lithologic components are highly stratified. Only two samples of the calcareous argillite subunit were available for measurement, thus evidence as to its textural and compositional character is inconclusive, but it does not appear to be very different from the overlying altered argillite. The lowermost marble unit has a high resistivity except where modified by high porosity.

With regard to other properties measured, perhaps the most significant is the high magnetic intensity of the altered argillite, which is sufficient to produce substantial magnetic anomalies when measured at the surface. The general level of variability recorded on all rock properties measured is the result of fracturing, alteration, and mineral reconstitution which accompanied and followed the localized doming of the Calico Hills by intrusive activity. This history of tectonic activity has produced rock types that are nonuniform in their textural qualities and are generally considered unsuitable for radwaste containment.

#### Selected References

- Anderson, L. A., Bisdorf, R. J., and Schoenthaler, D. R., 1980, Resistivity sounding investigation by the Schlumberger method in the Syncline Ridge area, Nevada Test Site, Nevada: U.S. Geological Survey Open-File Report 80-466, 21 p.
- Chleborad, A. F., Powers, P. S., and Farrow, R. A., 1975, A technique for measuring bulk volume of rock materials: Association of Engineering Geologists Bulletin, v. 12, no. 4, p. 307-312.
- Jahren, C. E., and Bath, G. D., 1967, Rapid estimation of induced and remanent magnetization of rock samples, Nevada Test Site: U.S. Geological Survey Open-File Report 67-122, 30 p.
- Johnson, Gordon R., 1979, Textural properties, in Hunt, G. R., Johnson, G. R., Olhoeft, G. R., Watson, D. E., and Watson, Kenneth, Initial report of the petrophysics laboratory: U.S. Geological Survey Circular 789, p. 67-74.
- Johnson, Gordon R., and Olhoeft, G. R., 1982, Density of rocks and minerals, in Handbook of physical properties of rocks, v. II: West Palm Beach, Fla., CRC Press, in press.
- Maldonado, Florian, Muller, D. C., and Morrison, J. N., 1979, Preliminary geologic and geophysical data of the UE25a-3 exploratory drill hole, Nevada Test Site, Nevada: U.S. Geological Survey report USGS-1543-6, 47 p.; available only from U.S. Department of Commerce National Technical Information Service, Springfield, VA 22161.
- Obert, Leonard, and Duvall, Wilbur I., 1967, Rock mechanics and the design of structures in rock: New York, London, Sydney, John Wiley & Sons, Inc., p. 344-350.
- Sumner, J. S., 1976, Principles of induced polarization for geophysical exploration: Amsterdam, Oxford, New York, Elsevier Scientific Publishing Co., 277 p.